

# Efficient 2.9 $\mu\text{m}$ fluorozirconate glass waveguide chip laser

David G. Lancaster,<sup>1,\*</sup> Simon Gross,<sup>2</sup> Heike Ebendorff-Heidepriem,<sup>1</sup> Michael J. Withford,<sup>2</sup>  
Tanya M. Monro,<sup>1</sup> and Stuart D. Jackson<sup>3</sup>

<sup>1</sup>*Institute for Photonics and Advanced Sensing (IPAS) and School of Chemistry and Physics, University of Adelaide, South Australia 5005, Australia*

<sup>2</sup>*CUDOS and MQ Photonics Research Centre, Department of Physics and Astronomy, Macquarie University, New South Wales 2109, Australia*

<sup>3</sup>*Institute of Photonics and Optical Science (IPOS), School of Physics, University of Sydney, Camperdown 2006, Australia*

\*Corresponding author: david.lancaster@adelaide.edu.au

Received May 20, 2013; revised June 18, 2013; accepted June 18, 2013;  
posted June 19, 2013 (Doc. ID 190759); published July 15, 2013

We report a large mode-area holmium-doped ZBLAN waveguide laser operating at 2.9  $\mu\text{m}$ , which was pumped by a 1150 nm diode laser. The laser is based on ultrafast laser inscribed depressed cladding waveguides fabricated in uniformly rare-earth-doped bulk glass. It has a threshold of 28 mW and produced up to 27 mW of output power at an internal slope efficiency of approximately 20%. © 2013 Optical Society of America

OCIS codes: (140.3070) Infrared and far-infrared lasers; (140.3580) Lasers, solid-state; (140.3390) Laser materials processing; (230.7380) Waveguides, channeled.

<http://dx.doi.org/10.1364/OL.38.002588>

Miniaturizing laser sources to make them compatible with chip technology is creating new opportunities in sensing and high repetition-rate pulsed sources, and has strong potential for high volume production. To date, a number of emission wavelengths and host materials have been explored with the goal of creating highly efficient output in a high-quality beam. Microchip laser sources [1] offer a small laser arrangement and high efficiency, and utilize a heavily doped bulk crystal in a short-cavity with the laser mode defined by pump-induced thermal lensing. Recent efforts have centered on creating waveguides in the gain medium, with a similar size to microchip lasers, as the initial steps toward all-on-chip-based laser devices. A major part of this research effort is the further extension of the emission wavelength of miniature laser sources toward and into the mid-infrared [2]. For example, the use of  $\text{Tm}^{3+}$  ion doping in double-tungstates [3] and fluoride glasses [4] has created highly efficient and high power emission in the 2  $\mu\text{m}$  region of the spectrum. A key requirement from the host in these examples is the capacity for high rare earth ion doping that can facilitate short absorption depths and efficient cross relaxation without the detrimental effects of scattering. The use of ion beam milling or ultrafast laser inscription (ULI) for the creation of the waveguide provides a sufficient refractive index difference between the guiding region and the surrounding cladding to allow minimal propagation loss in combination with good beam quality.

In this Letter, we extend these investigations of ultra-compact waveguide laser research to the demonstration of laser emission at 2.9  $\mu\text{m}$  using a ZBLAN glass host. The use of ZBLAN ( $\text{ZrF}_4$ ,  $\text{BaF}_4$ ,  $\text{LaF}_4$ ,  $\text{AlF}_3$ ,  $\text{NaF}_3$ ) glass combines the properties of high dopant concentration and low background loss with low phonon energy which is essential for laser emission beyond 2  $\mu\text{m}$ . In this initial demonstration, the  $\text{Ho}^{3+}$  ion was chosen as the laser ion because it naturally lases at longer wavelengths when

compared to the equally efficient  $\text{Er}^{3+}$  ion. Holmium is excited using readily available 1150 nm diode lasers. Measurements of the ESA spectrum [5] indicate that the  $\text{Ho}^{3+}$  ion suffers from less ESA when compared to the  $\text{Er}^{3+}$  ion pumped at 976 nm. Pump ESA is an important consideration in miniature waveguide laser research because the pump light illuminates, with a significant intensity, the core region of the waveguide. In previous studies of core-pumped  $\text{Er}^{3+}$ -doped ZBLAN fiber lasers [6], detrimental co-lasing at 850 nm populates the lower laser level of the 2.7  $\mu\text{m}$  transition causing saturation of the 2.7  $\mu\text{m}$  output.

The waveguide laser architecture we have developed for the current demonstration involves directly writing the waveguide using ULI to produce low-loss depressed-cladding waveguides in rare-earth-doped ZBLAN glass. The ULI process using MHz repetition rates creates a region of reduced refractive index ( $\Delta n \sim 0.001$ ) in this glass [7] that can be built up over multiple passes to form an annular cladding that surrounds an unmodified core as shown in Fig. 1(a). The resultant low loss ( $<0.4 \pm 0.2$  dB/cm) waveguide has been used to demonstrate chip-sized devices incorporating thulium and holmium ions for highly efficient laser emission at 1.9  $\mu\text{m}$  [8] and 2.1  $\mu\text{m}$  [9], respectively. The 1150 nm diode laser pumped  $\text{Ho}^{3+}$  waveguide laser we report here has achieved up to 27 mW output power at 2.9  $\mu\text{m}$  with a threshold of 28 mW and a 20% internal slope efficiency (SE). This is the longest wavelength reported for a chip-scale laser. Recent interest in extending the wavelength of emission from chip-scale devices [10] is driven by the large number of opportunities in sensing.

The 2.9  $\mu\text{m}$   $\text{Ho}^{3+}$  ion transition, see Fig. 1(b), is pumped directly into the upper laser level using 1150 nm diode lasers. The 2.9  $\mu\text{m}$  transition is burdened with an upper state ( $^5\text{I}_6$ ) lifetime of 3.5 ms that is shorter than the lower level ( $^5\text{I}_7$ ) lifetime of 12 ms [11]. In fiber laser research, co-lasing the  $^5\text{I}_7$  to  $^5\text{I}_8$  laser transition at 2.1  $\mu\text{m}$

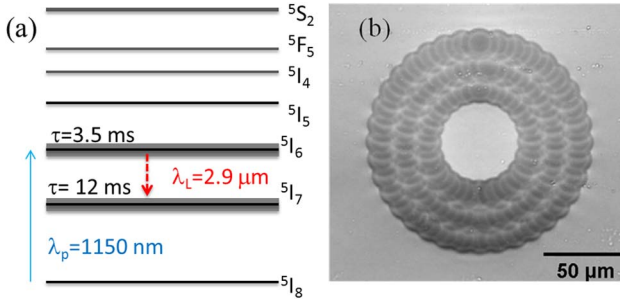


Fig. 1. (a) Energy level diagram of  $\text{Ho}^{3+}$  in ZBLAN glass. (b) End-on microscope image of the waveguide.

[12] or co-doping with  $\text{Pr}^{3+}$  ions has demonstrated unsaturated emission from the  $^5\text{I}_6$  to  $^5\text{I}_7$  laser transition at 2.9  $\mu\text{m}$ . For the present demonstration, we configured the waveguide cavity for cascade lasing by employing mirrors that provide a high quality resonator for both the 2.05 and 2.9  $\mu\text{m}$  emission wavelengths.

The  $\text{Ho}^{3+}$ -doped ZBLAN glass block was fabricated in-house in a dry atmosphere glass melting glovebox. The 50 g glass batch of nominal composition (in mol. %)  $53\text{ZrF}_4 - 20\text{BaF}_3 - 2.1\text{LaF}_3 - 1.9\text{HoF}_3 - 3\text{AlF}_3 - 20\text{NaF}$  was prepared in a glovebox purged with dry  $\text{N}_2$  ( $\leq 10$  ppmv water) using commercially available raw materials (anhydrous fluorides) of 99.9% or higher purity. The glass batch was melted in a platinum crucible within a silica liner that was located inside a tube furnace. The furnace liner was attached to the glovebox in a gas-tight configuration, and was (independently of the glovebox) purged with dry gas ( $\text{N}_2$ ,  $\text{O}_2$ , and/or  $\text{SF}_6$ ). The glass was first melted at 800°C for 2 h and then refined at 850°C for 0.5 h. For both melting and refining, the furnace liner was purged with a mixture of 80%  $\text{N}_2$  and 20%  $\text{O}_2$ . After refining, the glass melt was held at 750°C for 0.5 h in 96%  $\text{N}_2$  and 4%  $\text{SF}_6$  atmosphere to fluorinate the glass melt. Finally, prior to casting, the glass melt temperature was decreased to 650°C with  $\text{SF}_6$  purging switched off. The glass was then cast into a brass mould preheated to  $\sim 260^\circ\text{C}$ . The cast glass (within the brass mould) was annealed at 260°C for 1 h and then slowly cooled down to room temperature.

Previous melting trials using this procedure demonstrated that higher doping levels of 3 mol. % rare earth fluoride resulted in the formation of some crystals in the glass volume. Therefore, we restricted the  $\text{HoF}_3$  concentration to 1.9 mol. % in this work. The fabricated glass block was diced into rectangular chips (6 mm  $\times$  2.5 mm; lengths of 12 and 20 mm); the top and bottom surfaces were polished to optical grade. The measured pump absorption at the pump wavelength of 1150 nm was 3  $\text{dB cm}^{-1}$ .

Eight depressed-cladding waveguides of the form shown in Fig. 1(b) were inscribed into the doped glass with core diameters ranging from 25 to 52  $\mu\text{m}$  using ULI, as described in [8,9]. Numerical simulations, using the exact vectorial EM solution of an idealized depressed cladding waveguide, has shown that confinement loss (CL) of these “leaky mode” structures increases at longer wavelengths. To determine the CL, we determine the modal propagation constant ( $\beta$ ) by solving Maxwell’s equations for this waveguide geometry, and the

CL ( $\alpha$ ) determined by the relation  $\alpha_{\text{dB/cm}} = \text{Im}(\beta) \times 0.2 \times \log_{10}(e)$ .

In our previous thulium-doped waveguide laser operating at 1.9  $\mu\text{m}$  [8] we used a 22.5  $\mu\text{m}$  cladding made up of two interlocking rings of modifications which is predicted to have a CL of 0.7  $\text{dB/cm}$  at  $\lambda = 2.9 \mu\text{m}$ , which we consider too high to realize an efficient laser. Thus, to achieve low CL at  $\lambda = 2.9 \mu\text{m}$  a wider depressed cladding was required (as the typical ULI-induced  $\Delta n$  in ZBLAN is  $\sim -0.001$ ) [7]. Numerical simulations predicted that a 45  $\mu\text{m}$  cladding width surrounding a 52  $\mu\text{m}$  diameter core enabled the CL to be reduced to 0.08  $\text{dB cm}^{-1}$ .

To achieve a wider depressed cladding of  $\sim 45 \mu\text{m}$  a third ring of low index “rods” was written by ULI, giving 84 rods in total per waveguide. A microscope image of the resulting waveguide structure is shown in Fig. 1(b). The structure was built up from the lower (with respect to the photograph) part of the cladding. To avoid clipping of the highly converging ULI beam, the waveguides are only written to within  $\sim 250 \mu\text{m}$  of the ends of the sample, and then the ends are polished back to expose the waveguides.

Figure 2 shows a schematic of the experimental setup. The pump source, a continuous-wave 1150 nm diode laser (Ferdinand-Braun-Institut, Berlin), was free-space coupled into a 25  $\mu\text{m}$  core diameter, 0.1 NA fiber. The fiber output was coupled into the waveguide using two AR-coated plano-convex lenses ( $f = 35 \text{ mm}$  and  $f = 60 \text{ mm}$ ), giving a predicted pump spot size of  $\sim 43 \mu\text{m}$ . The largest 52  $\mu\text{m}$  diameter waveguide performed best for this pump launch condition and was thus used throughout the demonstration.

Flat dielectric-coated cavity mirrors were butted against each end of the uncoated chip. The input-coupler was highly transmitting at 1150 nm, and highly reflecting at the expected holmium laser emission wavelengths of 2.05 and 2.9  $\mu\text{m}$ . The output coupler (OC) was highly reflecting at 1150 nm, and  $R \sim 95\%$  at  $\lambda = 2.05$  and 2.9  $\mu\text{m}$ . To reduce the substantial Fresnel losses from the end faces of the chip, an anti-reflection coating had been applied by an external vendor, however, this failed to meet the transmission specification and had to be removed by repolishing. Alternatively, we investigated the use of a thin film of index matching oil (York) that was highly transmitting but with the drawback of  $n \sim 1.62$  (cf. ZBLAN  $n \sim 1.49$ ). We observed reduced efficiency of the laser when index matching oil was used on the pump input side of the resonator (compared to the uncoated efficiency) which we attribute to the high pump intensity causing degradation of the oil. When oil was applied on

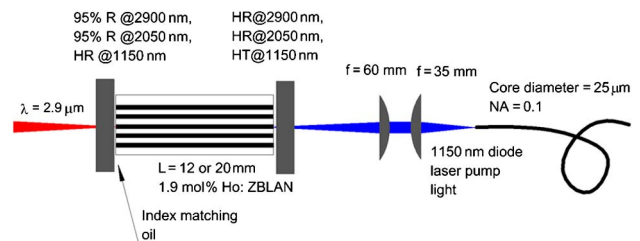


Fig. 2. Schematic of the 1150 nm diode-laser-pumped  $\text{Ho}^{3+}$ -ZBLAN laser.

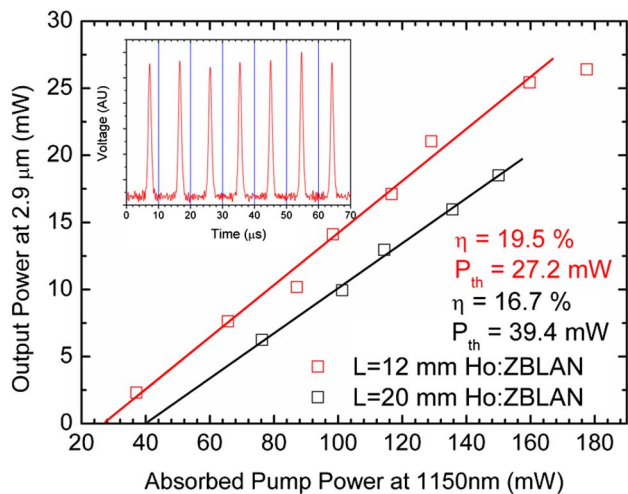


Fig. 3. Internal SE of the chip laser. The inset shows the temporal characteristic of the output from the CW pumped laser taken at  $P = 12$  mW (VIGO PEM, risetime  $< 1$  ns).

the OC end of the chip, the laser performance improved as a result of reduced Fresnel reflections ( $\sim 0.2\%$  per surface).

The SEs as a function of the absorbed pump power for the  $L = 12$  and  $20$  mm waveguides are shown in Fig. 3. The maximum SE was  $19.5\%$  for the  $L = 12$  mm waveguide. For this arrangement, the threshold was  $28$  mW and the maximum output power was  $27$  mW, which was reached at  $177$  mW of absorbed pump power. The SE (as a function of the incident power) for the  $12$  mm chip was  $15.9\%$ ; for the  $L = 20$  mm chip the SE was  $16.7\%$ , which is consistent with greater intra-cavity waveguide loss due to the increased chip length.

The inset to Fig. 3 shows the pulsed output from the laser recorded with a  $< 1$  ns risetime detector and a  $300$  MHz bandwidth oscilloscope. A regular train of  $\sim 1$   $\mu$ s wide pulses were observed at an output power of  $5$  mW and had a period of  $\sim 9.5$   $\mu$ s. This measurement was taken when no index matching gel was used. At an power output of  $11$  mW the pulse period decreased to  $3.5$   $\mu$ s. The repetition rate dependence on output power suggests the pulses relate to the relaxation oscillation frequency of the laser, however, further tests are required to isolate the underlying pulsing mechanism. No laser emission was detected at  $\sim 2$   $\mu$ m, indicating that cascade lasing did not reach threshold at the available pump power levels. Laser emission on the  ${}^5I_6$  to  ${}^5I_7$  transition at  $\sim 2.9$   $\mu$ m displayed a broad spectral feature (see Fig. 4) with the central wavelength shifting to longer wavelength with increased pump power. This is characteristic of a gradually filling terminal laser manifold which indicates that the lower laser level was filling toward a bottleneck. The beam profile (see inset to Fig. 4), taken using a Ophir pyrocam, was approximately Gaussian, indicating that the laser was operating single transverse mode. Due to beam degradation caused by coherent interference from our plane parallel polished Ge filter, no beam-quality measurement was carried out in this work.

The present demonstration represents the longest emission wavelength from a waveguide chip-scale laser

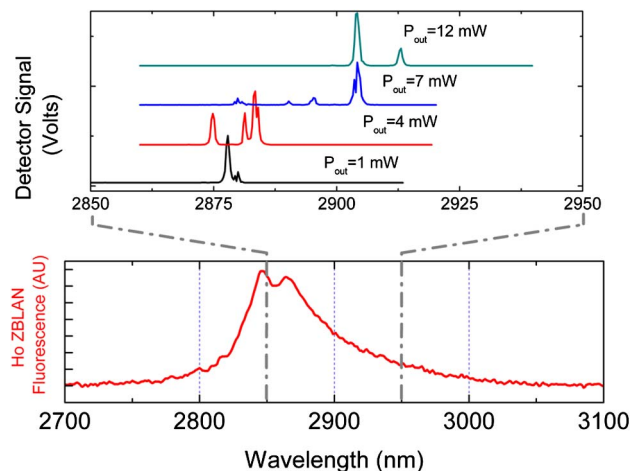


Fig. 4. (Top) Recorded spectra from the Ho: ZBLAN chip laser, showing modest wavelength shifts into the red for higher output powers. (Bottom) Recorded fluorescence spectrum collected transversely from a  $640$  nm excited  $\text{Ho}^{3+}$ : ZBLAN bulk sample. Inset is an image of the  $2.9$   $\mu$ m laser mode emitted from the waveguide laser.

and represents the initial steps toward the generation of an on-chip pulsed mid-infrared laser device. The use of ZBLAN glass combines a number of favorable qualities such as low scattering loss, low phonon energy, high rare earth ion solubility and ease of manufacture. We note that no evidence of degradation of the polished ZBLAN surfaces has been observed over several years, despite no special handling or storage precautions.

In conclusion, we report the longest wavelength planar waveguide laser. The laser operated near  $2.9$   $\mu$ m, emitted  $27$  mW with a  $\sim 20\%$  optical-to-optical SE, and a threshold of  $28$  mW. Compact high beam-quality chip lasers at this wavelength have the potential to underpin portable spectroscopic sensors, and the waveguide architecture is suitable for the development of mid-infrared photonic circuits.

This work was produced with the assistance of the Australian Research Council (ARC) under the Centres of Excellence, Linkage Infrastructure, Equipment and Facilities programs. T. Monro acknowledges the support of an ARC Federation Fellowship. S. Jackson acknowledges the support of an ARC Queen Elizabeth II Fellowship. Kenton Knight is acknowledged for ZBLAN glass fabrication and Darren Hudson is acknowledged for assisting with the laser demonstration. The devices were fabricated in the OptoFab node of the Australian National Fabrication Facility.

## References

1. J. J. Zayhowski and C. Dill III, *Opt. Lett.* **19**, 1427 (1994).
2. S. D. Jackson, *Nat. Photonics* **6**, 423 (2012).
3. K. van Dalzen, S. Aravazhi, C. Grivas, S. M. García-Blanco, and M. Pollnau, *Opt. Lett.* **37**, 887 (2012).
4. D. G. Lancaster, S. Gross, H. Ebendorff-Heidepriem, K. Kuan, T. M. Monro, M. Ams, A. Fuerbach, and M. J. Withford, *Opt. Lett.* **36**, 1587 (2011).
5. A. Felipe, H. Librantz, S. D. Jackson, L. Gomes, S. José Lima Ribeiro, and Y. Messaddeq, *J. Appl. Phys.* **103**, 023105 (2008).

6. S. Bedö, M. Pollnau, W. Lüthy, and H. P. Weber, *Opt. Commun.* **116**, 81 (1995).
7. S. Gross, D. G. Lancaster, H. Ebendorff-Heidepriem, T. M. Monro, A. Fuerbach, and M. J. Withford, *Opt. Mater. Express* **3**, 574 (2013).
8. D. G. Lancaster, S. Gross, A. Fuerbach, H. Ebendorff-Heidepriem, T. M. Monro, and M. J. Withford, *Opt. Express* **20**, 27503 (2012).
9. D. G. Lancaster, S. Gross, H. Ebendorff-Heidepriem, A. Fuerbach, M. J. Withford, and T. M. Monro, *Opt. Lett.* **37**, 996 (2012).
10. X. Gai, D. Y. Choi, S. Madden, Z. Yang, R. Wang, and B. Luther-Davies, *Opt. Lett.* **37**, 3870 (2012).
11. L. Wetenkamp, G. F. West, and H. Tobben, *J. Non-Cryst. Solids* **140**, 35 (1992).
12. T. Sumiyoshi and H. Sekita, *Opt. Lett.* **23**, 1837 (1998).